Nuclear Science and Techniques **24** (2013) 050516

Competition between fusion-evaporation and multifragmentation in central collisions in ^{58}Ni+^{48}Ca at 25*A* MeV

FRANCALANZA L[1,2,*] ABBONDANNO U[3] AMORINI F[1,2] BARLINI S[4] BINI M[4] BOUGAULT R[5] BRUNO M[6] CARDELLA G[7] CASINI G[8] AGOSTINO M D'[6] De FILIPPO V[7] De SANCTIS J[6] GERACI E[2,7] GIUSSANI A[9] GRAMEGNA F[10] GUIOT B[6] KRAVCHUK V[10] La GUIDARA E[11] LANZALONE G[1,12] Le NEINDRE N[5] MAIOLINO C[1] MARINI P[6] MORELLI L[6] OLMI A[8] PAGANO A[7] PAPA M[7] PIANTELLI S[8] PIRRONE S[7] POLITI G[2,7] POGGI G[4] PORTO F[1,2] RUSSOTTO P[1,2] RIZZO F[1,2] VANNINI G[6] VANNUCCI L[10]

[1]*INFN Laboratori Nazionali del Sud-LNS, Catania 95123, Italy*

[2]*Dipartimento di Fisica, Università di Catania I-95129, Italy*

[3]*INFN Sezione di Trieste, Trieste I-34127, Italy*

[4]*Dipartimento di Fisica, Università di Firenze, INFN Sezione di Firenze 1-50139, Italy*

[5]*LPC Caen, IN2P3-CNRS/ENSICAEN and Université, F-14050 Caen cedex 5-14076, France*

[6]*Dipartimento di Fisica, Università di Bologna and INFN Sezione di Bologna 4-50121, Italy*

[7]*INFN Sezione di Catania I-95129, Italy*

[8]*INFN Sezione di Firenze I-50139, Italy*

[9]*Dipartimento di Fisica, Università di Milano and INFN Sezione di Milano1-20126, Italy*

[10]*INFN Laboratori Nazionali di Legnaro 1-35020, Italy*

[11]*Centro Siciliano di Fisica Nucleare e Struttura della Materia, Catania 1-95129, Italy*

[12]*Università Kore, Enna 1-94100, Italy*

Abstract The experimental data concerning the ^{58}Ni+^{48}Ca reaction at E_{lab}(Ni)=25*A* MeV, collected by using the CHIMERA 4π device, have been analyzed in order to investigate the competition among different reaction mechanisms for central collisions in the Fermi energy domain. As a main criterion for centrality selection we have chosen the flow angle (ϑ_{flow}) method, making an event-by-event analysis that considers the shape of events, as it is determined by the eigenvectors of the experimental kinetic-energy tensor. For the selected central events (ϑ_{flow}>60°) some global variables, good to characterize the pattern of central collisions have been constructed. The main features of the reaction products were explored by using different constraints on some of the relevant observables, like mass and velocity distributions and their correlations. Much emphasis was devoted, for central collisions, to the competition between fusion-evaporation processes with subsequent identification of a heavy residue and a possible multifragmentation mechanism of a well defined (if any) transient nuclear system. Dynamical evolution of the system and pre-equilibrium emission were taken into account by simulating the reactions in the framework of transport theories. Different approaches have been envisaged (dynamical stochastic BNV calculations + sequential SIMON code, QMD, CoMD, etc.). Preliminary comparison of the experimental data with BNV calculations shows reasonable agreement with the assumption of sequential multifragmentation emission in the mass region of IMFs close to the heavy residues. Possible deviations from sequential processes were found for those IMFs in the region of masses intermediate between the mass of heavy residues and the mass of light IMFs. Further simulations are in progress. The experimental analysis will be enriched also by information obtained inspecting the IMF–IMF correlation function, in order to elucidated the nature of space-time decay property of the emitting source associated with events having the largest IMF multiplicity.

Key words Heavy ion collisions, Intermediate energy, Flow angle, Fusion-evaporation, Multifragmentation

* Corresponding author. *E-mail address:* laura.francalanza@ct.infn.it

Received date: 2013-06-27

1 Introduction

The study of nuclear reaction mechanisms in heavy-ion collisions at medium energies, i.e., at energies around the Fermi domain (~40 MeV/nucleon) is an unique way to investigate the competition among different nuclear processes, expected to play a competitive role in the transition from a mean field dissipation mechanism (one-body dissipation), dominating at bombarding energy close to the Coulomb barrier between the two interacting nuclei, to the nucleon-nucleon collision process (two body dissipation) that is the dominant mechanism in the relativistic domain.

In the past, one clear experimental signature of this transition mechanism was the observation of large values of the Intermediate Mass Fragments' (IMF, fragments with charge Z>2) multiplicity, especially in central collisions, that was more than one order of magnitude larger than that expected in the de-excitation of an equilibrated nuclear system at normal density produced in fusion-evaporation reactions at lower bombarding energy[1].

In order to explain this multi-fragmentation phenomenon, typically observed in central collisions, different reaction models, ranging from prompt dynamical emissions, simulated in the contest of transport theories, to statistical multifragmentation emissions of a (supposed) low density and short lived nuclear system at chemical equilibrium, were envisaged[1]. However, multiple emission of fragments has been also observed in semi-central collisions; so experimental studies of multifragmentation processes under several experimental conditions are also important in order to disentangle among different reaction mechanisms ranging from the quasi-elastic to the most dissipative collisions, as a function of the impact parameter.

In this paper, emphasis is given to characterize collisions at small impact parameters, where the maximum transferred linear momentum and the formation of single highly excited sources are expected to occur. So, a careful selection of central collisions in the reaction ^{58}Ni+^{48}Ca[2] is described in order to pin down the competition between sequential fusion-evaporation decay and prompt multifragmentation emission of an unstable system formed at sub-saturation nuclear density.

2 Experiment

The experiment was performed by the NUCLEX-ISOSPIN collaboration and it was realized with the CHIMERA apparatus, located at LNS–INFN (Catania).

A beam of ^{58}Ni ions was accelerated at 25A MeV energy on a thin target of ^{48}Ca by the LNS Superconducting Cyclotron, and the reaction products were collected by the 1192 Si-CsI(Tl) telescopes of CHIMERA 4π multidetector, covering almost 94% of the total solid angle[2,3]. Events were collected when at least two Silicon detectors were fired, i.e. when the charged particle multiplicity (M_{CP}) was larger than two hits (M_{CP}≥2).

By means of the ΔE–E identification technique, it was possible to determine the atomic number Z of the reaction products punching through the silicon (n-planar-300 μm) detector and stopped in the CsI(Tl) crystal as well as the charge and mass of those IMFs with 3≤Z≤8, detected at laboratory angles larger than 13°. Time-of-flight (TOF) technique provided the measure of particles' velocity, by using the cyclotron radiofrequency reference time as start, and the silicon time signal as stop.

Then, combining the energy and the TOF information, it was possible to evaluate the mass of particles stopped in the first stage of telescopes.

In this analysis the Pulse Shape Discrimination (PSD) technique in CsI(Tl) , used for the identification of light charged particles (LCP), has not been performed, which, however, only slightly affects the global reconstruction of the reaction pattern, made on an event-by-event basis.

3 Event selection

The analysis was performed on the so called "complete events", selected by imposing that total detected charge, as well as total measured linear momentum, ranges between 70% and 105% of the total charge of the interacting system and the projectile's momentum, respectively. In this way, the

11.5% of total collected events has been selected (see region in square box in Fig.1).

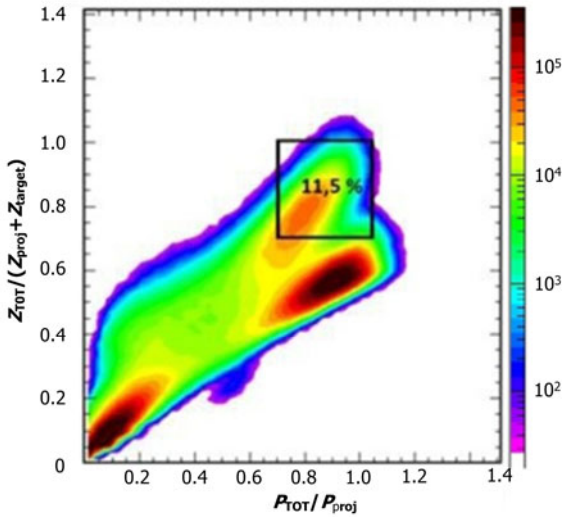

Fig.1 (Color online) Correlation between total detected charge and total longitudinal momentum for all detected events. Events in the square box (11.5 % of total events) were selected as complete events.

3.1 Centrality selection

The method adopted to perform a good selection of centrality is based on imposing several cuts on the global variable "flow angle", ϑ_{flow} , that is related to the shape of the event in momentum space[4-8]. This latter variable is built starting from the Cartesian coordinates of the measured linear momenta, in the centre of mass frame (CM), for all the fragments ($Z\geq3$) detected in each event. The kinetic flow tensor, Q_{ij}, is built event by event as follow:

$$Q_{ij} = \Sigma_{Z\geq3}\, p_i\, p_j /2m\ . \qquad (1)$$

This tensor is a generalization of the sphericity tensor, widely used in high energy particle physics and adapted to heavy-ions nuclear reactions in which composite fragments are produced. In its diagonal form Q_{ij} defines an ellipsoid in momentum space with the three principal axes oriented along the three eigenvectors, whose corresponding eigenvalues f_1, f_2 and f_3, are sorted and ordered according to the inequalities $f_1>f_2>f_3>0$[4,9-12]. The orientation of the main axis of the ellipsoid (eigenvector corresponding to f_1) measured with respect to the direction of the incident beam defines the flow angle ϑ_{flow}.

Flow angle assumes values ranging from 0 to 90 degrees. For peripheral and semi-peripheral collisions, where the events keep memory of the binary character of the reaction, the shape of the tensor is elliptic and ϑ_{flow} assumes small values (<<90 degrees), while for more central collisions a more spherical shape is predicted, so that ϑ_{flow} will assume larger values, up to values of 90 degrees.

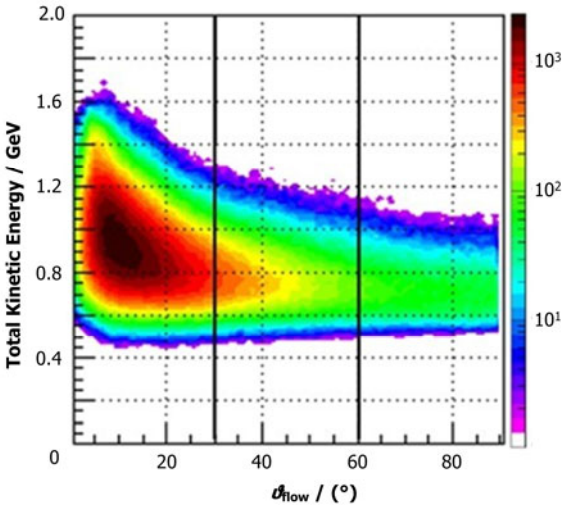

Fig.2 (Color online) Total Kinetic Energy (TKE) and ϑ_{flow} angle correlation, for all the complete events.

Figure 2 shows the correlation plot between the Total Kinetic Energy (measured by the sum of kinetic energy of all detected fragments in each event) and the flow angle variable[13]. An increase in ϑ_{flow} values results in a selection of more dissipative collisions.

Following the pattern of the emissions, in terms of the correlation between the longitudinal component (i.e. along the beam axis) of the velocity v_{par} and the mass number A, for each detected reaction product with increasing the value of the flow angle, we can notice that the contribution from fragments with velocity values close to projectile's velocity (v_{proj} =6.5 cm·ns^{-1}) and masses around 40–45 amu, indicated by the symbol PLF, and also from slow moving fragments corresponding to target's remnants, TLF, that are dominant at low flow angle values (close to zero degrees) and strongly indicative for binary peripheral collisions, is progressively reduced, until it completely vanishes at high values of ϑ_{flow} at 60 degrees and beyond (Fig.3).

Moreover, in the region of flow angle larger than 60 degrees, the longitudinal velocity spectrum is more and more centered around the value of v_{CM} , and a relevant emission component due to fragments with mass values larger than those of projectile or target,

also exceeding 60 amu, is clearly observed.

So, in the following, we will refer to events in the third region of flow angle ($\vartheta_{flow}\geq60°$) as central events[7], that cover the 6.2% of the complete events.

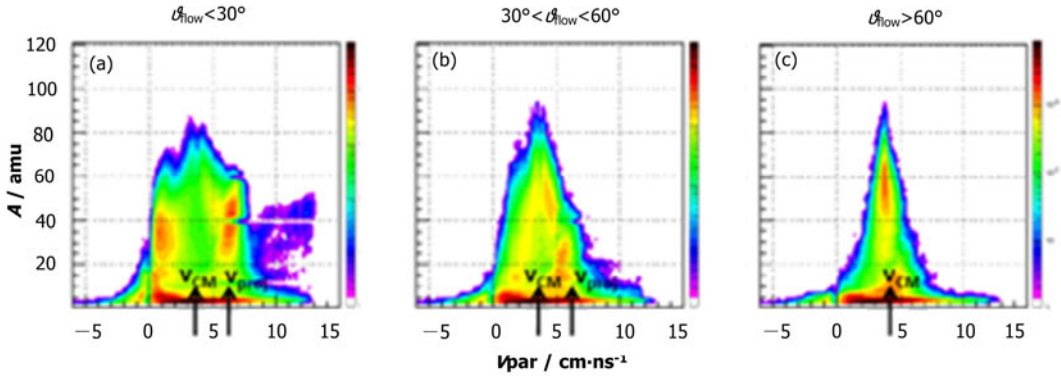

Fig.3 (Color online) Correlation between parallel velocity component (cm/ns) and mass (amu) for all reaction products in the three regions: $\vartheta_{flow}\leq0°$ (a), $30°<\vartheta_{flow}\leq60°$ (b) and $\vartheta_{flow}>60°$ (c).

3.2 Central events: event by event analysis

In these central collisions we first analyze the behavior of the heaviest fragment (A_{big}) in each event. We notice a broad distribution of A_{big} mass values, ranging from about 20 amu up to values around 80 amu (Fig.4). Typically, the class of events with the largest values of the A_{big} (50–80 amu) is reminiscent of a heavy residue formation following a fusion-like evaporation mechanism where the decay chain is dominated by the emission of light charged particle LP, *n*, gamma rays and few light fragments. To what extend the lower values of A_{big} (less than 30–40 amu) could be also produced in a fusion evaporation mechanism will be discussed in the following. However, the presence of events characterized by such a lower mass values of the heaviest fragment is a good candidate for an experimental signature of the possible coexistence of statistical fusion-like evaporation decay mechanism and a "prompt" multifragmentation process.

So, in order to disentangle between these two mechanisms, we chose to analyze two classes of events, imposing preliminarily an arbitrary cut at a value of the mass of the heaviest fragment equal to 50 amu. In order to better characterize our choice, the mean values of IMFs multiplicity, $<M_{IMF}>$, and the mean values of LP multiplicities, $<M_{LP}>$, are shown in the inset of Fig.4 for both the two classes of fragments.

The biggest fragment with mass 50 amu or larger is preferentially emitted as a unique heavy fragment (43.5% of events in the upper box of Fig.4) in coincidence with 4–5 light charged particles (Z=1, Z=2) or, alternatively, together with a few (1–2) light fragments; in contrast, by inspecting the lower box of Fig.4, it is seen that the fragment multiplicity M_{IMF} spans a substantially wider range of values, with a mean of $<M_{IMF}>$=3, and reaching maximum values as high as M_{IMF}=6. It has to be noted that for these latter events, the light charged particle multiplicity is lowered to a mean value of about three particles per event.

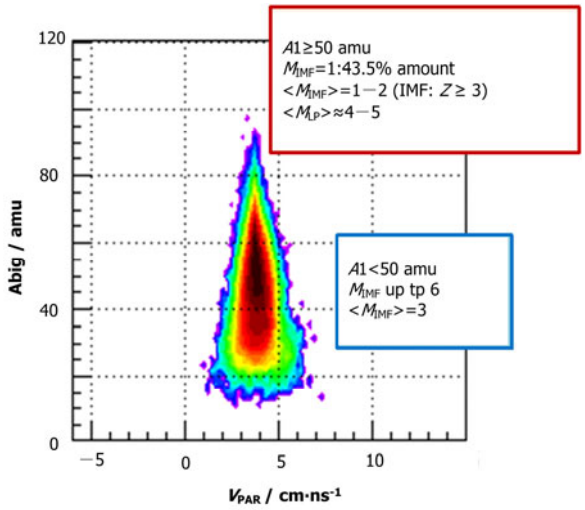

Fig.4 (Color online) Mass (amu) and longitudinal velocity (cm/ns) for the heaviest fragment for central events.

Complementary observation of the behavior of the two classes of events comes from the analysis of Dalitz plots in Fig.5. We briefly remind the reader that each reaction event corresponds to a point in the Dalitz Plot of Fig.5, and that the position of each point (event) inside the triangle gives information about the relative asymmetry in mass of the three heaviest fragments: in

the vertex are located events with a heavy residue, the sides are occupied by events characterized by a binary behavior (more or less symmetric splitting) and at the centre of this triangle are located events with a multi-fragmentation emission of fragments with nearly equal mass.

Looking at the left panel of Fig.5 (class of events with mass of A_{big}>50 amu), we can observe that mostly of the events are located on the vertices of plot, indicating the dominance of a heavy residue and light particles, that displays the characteristic features of typical fusion-evaporation phenomena. Otherwise, events in the right panel (class of events with mass of A_{big}<50 amu) show the approaching of a more symmetric splitting of the primary source, filling the area inside the triangle and, so, depleting vertex and sides.

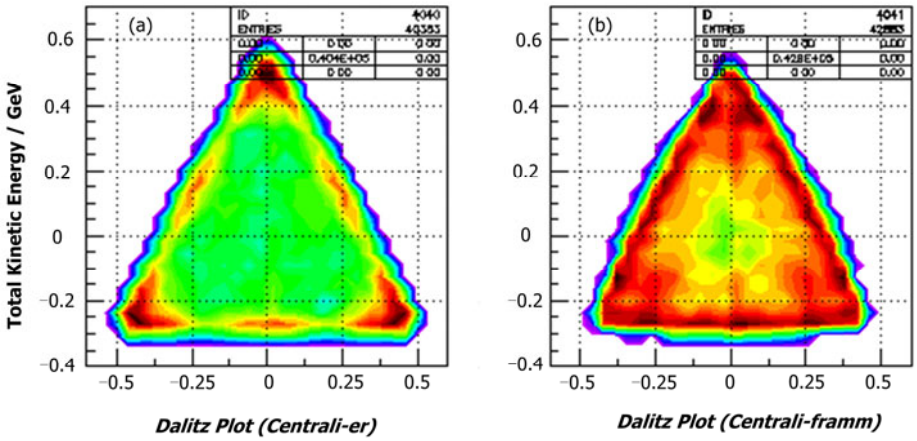

Fig.5 (Color online) Dalitz Plot for events in Fig.4.

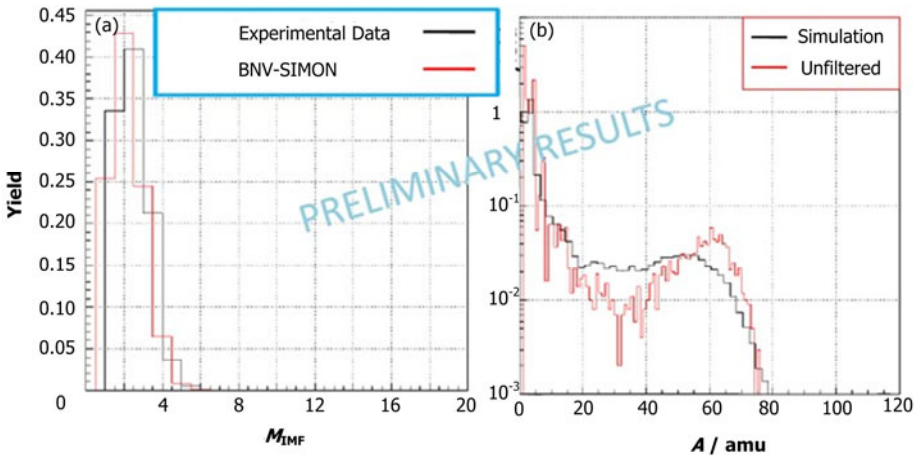

Fig.6 (Color online) Comparison between experimental and simulated M_{IMF} distribution. Mass distribution for experimental data (a) and results of simulation (b).

4 Comparison and calculation

We have compared mass distributions and multiplicities for selected central events (without any differentiation among fusion-evaporation and multifragmentation like events) with those predicted by a two step mechanism: dynamical stochastic BNV calculation followed by the sequential de-excitation of a composite source (SIMON code)[14]. The source information was obtained from BNV calculation, including pre-equilibrium emission of about 20 amu, and so corresponding to a source with mass equal 94 amu, charge of atomic number Z=43 and an excitation energy equal to 400 MeV (±50 MeV). In this calculations we have considered, as preliminary evaluation, only events produced in central collisions of vanishing angular momentum (L=0).

Figure 6 shows the comparison between fragment multiplicity distributions (left panel) and between mass distributions (right panel) for experimental data (black line) and for the calculations (red line). At this stage of the comparison the results of the simulation are not yet filtered, i.e., energy and mass resolutions, detector efficiency and trigger threshold are not included. We notice the quite good agreement in reproducing the shape of the multiplicity distribution. Taking into account that the effects of filtering (not yet included) are expected to change the shape of the calculated distribution mostly in the region of large values of the mass number A, the experimental data for both heavy and light reaction products are also well reproduced. Deviation (if any) from simulated and experimental mass distribution are located around mass values of about 30 amu.

5 Conclusion and perspective

The experimental data of ^{58}Ni+^{48}Ca reactions at E_{lab}(Ni)=25A MeV, collected by using the CHIMERA 4π device, have been analyzed in order to investigate the competition among different reaction mechanisms for central collisions.

As main criterion for centrality selection we have chosen the flow angle method, making an event-by-event analysis that considers the shape of events in the momentum space. For the selected central events (ϑ_{flow}>60°), mass-velocity correlations, built for all emitted fragments show a typical broad mass spectrum centered at v_{CM} velocity. Beside a component of IMF with mass number A<20, we notice the presence of a well shaped quasi-gaussian component with high values of mass (50–80 amu) strongly indicating the formation of a heavy residue coming from a fusion-evaporation statistical decay process of highly excited compound nuclei at equilibrium.

By means of further analysis concerning the multiplicity of fragments (M_{IMF}) and of charged light particles (M_{LCP}), and the mass distribution of the heaviest fragment emitted in well selected central collisions, a possible signature for the coexistence of two different reaction mechanisms in the observed mass spectrum was investigated. The reaction dynamics was simulated by Stochastic BNV transport simulations, taking into account for pre-equilibrium emission, and subsequent statistical evaporation decay. Preliminary comparisons of the experimental data with the results of a reaction simulation in the frame of stochastic BNV model coupled, as second step, with a statistical evaporation model show reasonable qualitative agreement with the assumption of sequential multi-fragmentation emission. However, to test this preliminary conclusion, further comparisons with dynamical transport models based on different assumptions are needed. Calculations with dynamical molecular models (QMD-CoMD …) are also in progress.

Furthermore, an extension of present analysis to light charged particles is envisaged, in order to investigate relevant characterization of the emitting source, like temperature (investigating the slope of the spectra, T_{slope}, and by means of double ratio analysis, T_{ratio}, or isotopic ratio thermometer) as well as evaluations of excitation energy and nuclear density at the freeze out configuration.

Recently, the CHIMERA group is also working on an upgrade of the apparatus, in order to extend the revelation's capabilities towards the identification of both charged and neutral particle[15].

The experimental analysis will be enriched also by complementary information obtained inspecting IMF-IMF correlation functions, in order to elucidate nature of space-time decay properties of sources, and so to disentangle sequential *vs.* simultaneous emission[16].

References

1 Lynch W G. Nucl Phys A, 1995, **583:** 471–480.

2 Pagano A. Proposal for upgrading CHIMERA 4π detector. Proceeding XLII International Winter Meeting on Nuclear Physis, Bormio, Italy, March, 2005, 150–155.

3 Pagano A. Nucl Phys News, 2012, **22:** 25–30.

4 Cugnon J and L'hote D. Nucl Phys A, 1983, **397:** 519–543.

5 Geraci E and Trimarchi M. Proceeding of the IWM2009, International Workshop on Multifragmentation and related topics, Catania, Italy, November 2009, 30–36.

6 Francalanza L. Central collisions in 58Ni + 48Ca system with CHIMERA at 25A MeV", Il Nuovo Cimento, DOI 10.1393/ncc/i2012-11305-7, 2012.

7 Marie N, Laforest R, Bougault R, *et al.* Phys Lett B, 1997, **391:** 15–21.
8 D'Agostino M, Mastinu P F, Milazzo P M, *et al.* Phys Lett B, 1996, **368:** 259–265.
9 Gyulassy M, Frankel K A, Stocker H. Phys Lett B, 1982, **110:** 185–188.
10 Herrmann N, Wessels J P, Wienold T. Annu Rev Nucl Part Sci, 1999, **49:** 581–632.
11 Stocker H, Buchwald G, Graebner G, *et al.* Nucl Phys A, 1982, **387:** 205c–218c.
12 Stocker H and Greiner W. Phys Rep, 1986, **137:** 277–392.
13 Lecolley J F, Durand D, Aboufirassi M, *et al.* Phys Lett B, 1996, **387:** 460–465.
14 Durand D. Nucl Phys A, 1992, **266:** 54–59.
15 Pagano A. Invited Talk – National Conference SIF, 2012.
16 Verde G, Chbihi A, Ghetti R. Eur Phys J A, 2006, **30:** 81.